JACS
JOURNAL OF THE AMERICAN CHEMICAL SOCIETY

ARTICLE

pubs.acs.org/JACS

Pyranoside Phosphite−Oxazoline Ligands for the Highly Versatile and Enantioselective Ir-Catalyzed Hydrogenation of Minimally Functionalized Olefins. A Combined Theoretical and Experimental Study

Javier Mazuela,[†] Per-Ola Norrby,[*,‡] Pher G. Andersson,[*,§,∥] Oscar Pàmies,[†] and Montserrat Diéguez[*,†]

[†]Departament de Química Física i Inorgànica, Universitat Rovira i Virgili, Campus Sescelades, C/Marcel·lí Domingo, s/n. 43007 Tarragona, Spain

[‡]Department of Chemistry, University of Gothenburg, Kemigården 4, SE-412 96 Göteborg, Sweden

[§]Department of Biochemistry and Organic Chemistry, Uppsala University, Box 576, 751 23 Uppsala, Sweden

[∥]School of Chemistry, University of KwaZulu-Natal, Durban, South Africa

Supporting Information

ABSTRACT: A modular set of phosphite−oxazoline (P,N) ligands has been applied to the title reaction. Excellent ligands have been identified for a range of substrates, including previously challenging terminally disubstituted olefins, where we now have reached enantioselectivities of 99% for a range of substrates. The selectivity is best for minimally functionalized substrates with at least a moderate size difference between geminal groups. A DFT study has allowed identification of the preferred pathway. Computational prediction of enantioselectivities gave very good accuracy.

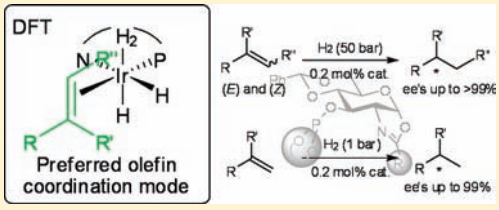

1. INTRODUCTION

Pharmaceuticals, agrochemicals, fragrances, fine chemicals, and natural chemicals all rely on the preparation of enantiomerically enriched compounds.[1] Because of its high efficiency, atom economy, and operational simplicity, the asymmetric hydrogenation of properly selected prochiral starting materials can be a sustainable and direct synthetic tool for preparing these compounds.[1]

Whereas the reduction of olefins containing an adjacent polar group (i.e., dehydroaminoacids) by Rh- and Ru-catalyst precursors modified with phosphorus ligands has a long history, the asymmetric hydrogenation of minimally functionalized olefins is less developed because these substrates do not have an adjacent polar group to direct the reaction.[1] Iridium complexes with chiral P,N ligands have become established as one of the most efficient catalyst types for the hydrogenation of minimally functionalized olefins, and they complement Rh− and Ru−diphosphine complexes.[2,3] The first successful P,N ligands[4] contained a phosphine or phosphinite moiety as P-donor group and either an oxazoline,[4b,g,j] oxazole,[4d] thiazole,[4i] or pyridine[4c] as N-donor group. However, these iridium−phosphine/phosphinite,N catalysts were still highly substrate-dependent, and the development of efficient chiral ligands that tolerate a broader range of substrates remained a challenge. In our efforts to expand the range of ligands and improve performance, we recently discovered that the presence of biaryl−phosphite moieties in these P,N-ligands provides greater substrate versatility than previous Ir−phosphine/phosphinite,N catalyst systems.[5] In this context, in 2008, we communicated the successful application of pyranoside phosphite−oxazoline ligands in the Ir-catalyzed asymmetric hydrogenation of model trisubstituted and terminal substrates.[5a] To fully investigate the potential of these ligands, in this Article we expand the 2008 study to other pyranoside phosphite−oxazoline ligands (Figure 1) and to other types of more challenging substrates. We have therefore extended the Ir−phosphite−oxazoline catalyst library by including pyranoside ligands with new substituents at the oxazoline (ligands **L4**) and at the biaryl phosphite group (**a**, **b**, **f**, **g**, and **j**). Ligands **L1**−**L5a**−**k** combine the advantages of phosphite and sugar cores: that is to say, they are readily available from cheap feedstocks and have high resistance to oxidation, and a straightforward modular construction.[6] With this ligand library, we can investigate the effect of systematically varying the electronic and steric properties of the oxazoline substituent (**L1**−**L5**) and different substituents and configurations in the biaryl phosphite moiety (**a**−**k**) with the aim to maximize catalyst performance. By judicious choice of the ligand components, we achieved high enantioselectivities and activities in a wide range of *E*- and Z-trisubstituted and 1,1-disubstituted alkenes.

Despite the recent success of Ir/phosphite−nitrogen catalyst systems, no mechanistic studies have been carried out on the hydrogenation of minimally functionalized alkenes using phosphite ligands. In this context, the mechanistic aspects of these

Received: May 30, 2011
Published: July 15, 2011

ACS Publications © 2011 American Chemical Society

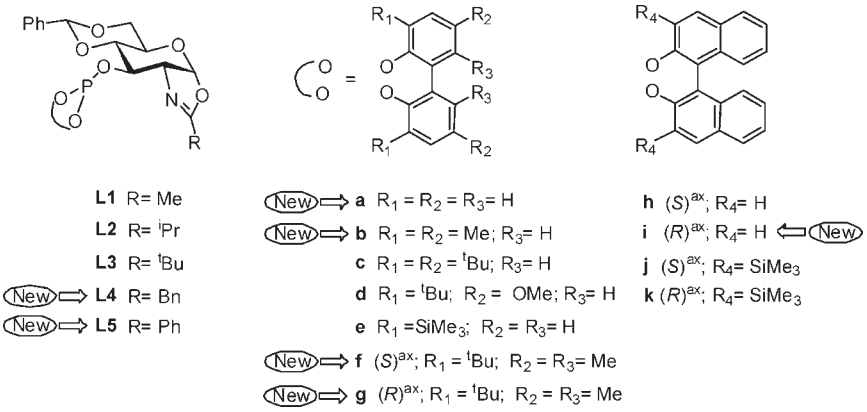

Figure 1. Pyranoside phosphite−oxazoline ligand library **L1**−**L5a**−**k**. In this work, the ligand library has been expanded by including new substituents at the oxazoline (**L4**) and at the biaryl phosphite moiety (**a**, **b**, **f**, **g**, and **i**).

Scheme 1. Synthesis of New Pyranoside Ligands

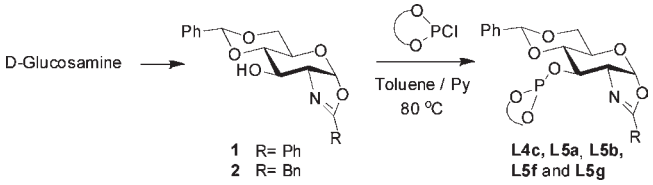

Scheme 2. Synthesis of Catalyst Precursors [Ir(cod)(P−N)] BAr_F (P−N = L1−L5a−k)

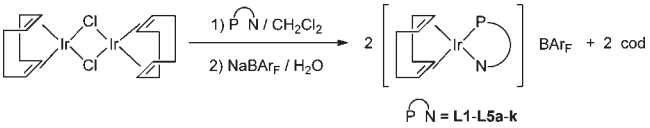

ligands are still not understood well enough for the a priori prediction of the type of ligand needed for high selectivity. To address this important point, in this Article we have also performed DFT calculations to explain the origin of enantioselectivity for these highly versatile pyranoside Ir/phosphite−oxazoline catalytic systems. It should be noted that we have also elucidated a computational model that can explain the enantioselectivities obtained with 1,1-disubstituted substrates, which was lacking in the literature.

2. RESULTS AND DISCUSSION

2.1. Synthesis of Ligands. The synthesis of the new pyranoside phosphite-oxazoline ligands (**L4c**, **L5a**, **L5b**, **L5f**, and **L5g**) is straightforward following the procedure previously described for ligands **L1**−**L3c**, **L5a**−**e**, and **L5h**−**k** (Scheme 1).[5a,7] They were therefore efficiently synthesized in one step by reacting the corresponding sugar oxazoline−alcohols (**1** and **2**) with 1 equiv of the corresponding biaryl phosphorochloridite ($ClP(OR)_2$; $(OR)_2$ = **a**−**c**, **f**, **g**) in the presence of pyridine, in a parallel way (see Experimental Section for details). Oxazoline−alcohols **1** and **2** are easily prepared from inexpensive D-glucosamine on a large scale.[8] All of the ligands were stable during purification on neutral alumina under an atmosphere of argon and isolated in moderate-to-good yields as white solids. They were stable at room temperature and very stable to hydrolysis. The elemental analyses were in agreement with the assigned structure. The ^1H, ^{13}C, and ^{31}P NMR spectra were as expected for these C_1 ligands.

2.2. Synthesis of the Ir-Catalyst Precursors. The catalyst precursors were made by refluxing a dichloromethane solution of the appropriate ligand (**L1**−**L5a**−**k**) in the presence of 0.5 equiv of $[Ir(\mu\text{-Cl})cod]_2$ for 1 h and then exchanging the counterion with sodium tetrakis[3,5-bis(trifluoromethyl)phenyl]borate ($NaBAr_F$) (1 equiv), in the presence of water (Scheme 2).[9] All complexes were isolated as air-stable orange solids and were used without further purification.

The complexes were characterized by elemental analysis and ^1H, ^{13}C, and ^{31}P NMR spectroscopy. The spectral assignments were based on information from $^1H-^1H$ and $^{13}C-^1H$ correlation measurements and were as expected for these C_1 iridium complexes. The VT-NMR spectra indicate that only one isomer is present in solution. One singlet in the $^{31}P\{^1H\}$ NMR spectra was obtained in all cases.[10]

2.3. Asymmetric Hydrogenation of Trisubstituted Olefins. *2.3.1. Asymmetric Hydrogenation of Minimally Functionalized Trisubstituted Olefins.* In a first set of experiments, we used the Ir-catalyzed hydrogenation of substrates *trans*-α-methylstilbene **S1** and *Z*-2-(4-methoxyphenyl)-2-butene **S2** to study the potential of ligands **L1**−**L5a**−**k**. Substrate **S1** was chosen as a model for the hydrogenation of *E*-isomers because it has been reduced with a wide range of ligands, which enable the efficiency of the various ligand systems to be compared directly.[2] To assess the potential of the ligand library **L1**−**L5a**−**k** for the more demanding *Z*-isomers, which are usually hydrogenated less enantioselectively than the corresponding *E*-isomers, we chose substrate **S2** as a model. The reactions proceeded smoothly at room temperature. Excellent activities and enantioselectivities (up to >99% for **S1** and up to 95% for **S2**) were obtained. The results, which are summarized in Table 1, indicate that activity is mainly affected by the steric properties of the oxazoline substituent and by the substituents at the *ortho* positions of the biaryl phosphite moiety. Bulky substituents need to be present in the biaryl phosphite and less sterically demanding substituents in the oxazoline if activities are to be high. Enantioselectivity, on the other hand, is affected by the electronic and steric properties of the substituents in the oxazoline moiety and by the substituents/configuration in the biaryl phosphite moiety. However, the effect

dx.doi.org/10.1021/ja204948k | J. Am. Chem. Soc. 2011, 133, 13634–13645

Table 1. Ir-Catalyzed Asymmetric Hydrogenation of S1 and S2 Using Ligands L1−L5a−k[a]

		S1		S2	
Entry	Ligand	% Conv[b]	% ee[c]	% Conv[b]	% ee[c]
1	**L1c**	100	92 (*R*)	100	69 (*S*)
2	**L2c**	98	95 (*R*)	100	73 (*S*)
3	**L3c**	40	99 (*R*)	44	75 (*S*)
4	**L4c**	100	98 (*R*)	100	85 (*S*)
5	**L5a**	32	96 (*R*)	58	75 (*S*)
6	**L5b**	<5	-	<5	-
7	**L5c**	100	99 (*R*)	100	95 (*S*)
8	**L5d**	100	98 (*R*)	100	79 (*S*)
9	**L5e**	100	>99 (*R*)	100	78 (*S*)
10	**L5f**	100	38 (*R*)	56	34 (*S*)
11	**L5g**	100	99 (*R*)	100	91 (*S*)
12	**L5h**	50	20 (*R*)	59	44 (*S*)
13	**L5i**	45	98 (*R*)	67	74 (*S*)
14	**L5j**	23	32 (*R*)	39	38 (*S*)
15	**L5k**	100	99 (*R*)	100	79 (*S*)
16[d]	**L5c**	100	99 (*R*)	100	95 (*S*)
17[d]	**L5e**	100	>99 (*R*)	100	78 (*S*)

[a] Reactions carried out by using 1 mmol of substrate and 2 mol% of Ir-catalyst precursor at 50 bar of H_2 using dichloromethane (2 mL) as solvent. [b] Conversion measured by ^{1}H-NMR after 2 h. [c] Enantiomeric excess determined by HPLC (**S1**) and GC (**S2**). [d] Reaction carried out at 0.2 mol% of Ir-catalyst.

of these ligand parameters on enantioselectivity depends on the substrate type (*E*- or *Z*-isomers). Thus, while for the *E*-substrate **S1** the enantioselectivity was best with ligand **L5e** (>99% ee), enantioselectivities for the more demanding *Z*-substrate **S2** were best with ligand **L5c** (95% ee). For both types of substrates, we also found a cooperative effect between the configuration of the biaryl phosphite moiety and the configuration of the sugar backbone on enantioselectivity. This led to a matched combination for ligands **L5g**, **L5i**, and **L5k**, which contain an *R*-biaryl moiety (entries 11, 13, and 15). In addition, a comparison of the absolute stereochemistry obtained by using tropoisomeric biphenyl ligands **L5a**−**e** with those obtained with the related atropoisomeric biaryl ligands (**L5f**−**k**) shows that the tropoisomeric biphenyl moiety in ligands **L5a**−**e** adopts an *R*-configuration when complexed with iridium.[10]

Next, we used the ligands that provided the best results (ligands **L5c** and **L5e**) to study these reactions at a low catalyst loading (0.2 mol %). In these conditions, the excellent enantioselectivities and activities were maintained (Table 1, entries 16 and 17).

We then studied the asymmetric hydrogenation of other *E*- and *Z*-trisubstituted olefins (**S3**−**S10**) by using the pyranoside

Scheme 3. Selected Hydrogenation Results of Trisubstituted Olefins Using [Ir(cod)(L1−L5a−k)]BAr$_F$ Catalyst Precursors[a]

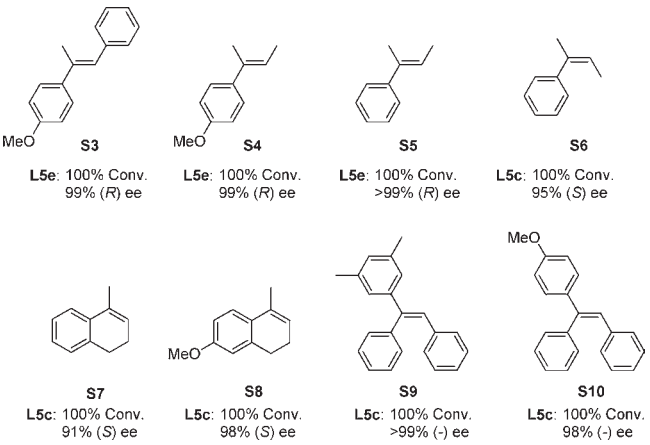

[a] Reaction conditions: 1 mol % catalyst precursor, CH_2Cl_2 as solvent, 50 bar H_2, 2 h.

phosphite−oxazoline ligand library **L1**−**L5a**−**k**. The most noteworthy results are shown in Scheme 3. The enantioselectivities are among the best observed for these substrates.[2,4] In general, the Ir−**L5e** catalyst precursor provides the best enantioselectivities for the hydrogenation of *E*-trisubstituted olefins (**S1**, **S3**−**S5**), while ligand **L5c** gives the best enantioselectivities for *Z*-trisubstituted olefins (**S2**, **S6**−**S8**). Our results also indicated that enantioselectivity (ee values up to >99%) is relatively insensitive to the electronic nature of the substrate phenyl ring (i.e., substrates **S1**, **S5**, and **S6** versus **S3**, **S4**, and **S2**, respectively). Notably the [Ir(cod)(**L1**−**L5a**−**k**)]BAr$_F$ catalyst precursors also proved to be highly active and enantioselective in the reduction of triarylsubstituted substrates **S9** and **S10** (Scheme 3, ee's ranging from 98% to >99%). This latter substrate class provides an easy entry point to diarylmethine chiral centers, which are present in several important drugs (such as (*R*)-tolterodine and sertraline) and natural products (i.e., podohyllotoxin).[11] Despite this, only one previous study has been made using Ir-catalysts modified with chiral phosphine/thiazole ligands (ee's up to 99%).[12]

2.3.2. Asymmetric Hydrogenation of Trisubstituted Olefins Containing a Neighboring Polar Group. To further study the potential of the pyranoside phosphite−oxazoline ligand library **L1**−**L5a**−**k** in the reduction of minimally functionalized trisubstituted olefins, we screened it in the Ir-catalyzed hydrogenation of trisubstituted alkenes containing a neighboring polar group. These substrates are interesting because they allow for further functionalization, and they are important intermediates for the synthesis of high-value chemicals. The results are summarized in Scheme 4. Again, excellent enantioselectivities (ee values up to >99%) for a range of substrates were obtained under mild reaction conditions. The reduction of several α,β-unsaturated esters (**S11**−**S14**) followed the same trends as those observed for the previous *E*-trisubstituted substrates. Therefore, enantioselectivities were best using ligand **L5e**. It should be noted that ee's are highly independent of the electronic nature of the substrate phenyl ring and the substituent in the ester functionality. As expected, the hydrogenation of vinylsilane **S15** was also best using ligand **L5e**. However, for trisubstituted allylic alcohol

Scheme 4. Selected Hydrogenation Results of Trisubstituted Olefins Bearing a Neighboring Polar Group Using [Ir(cod)(L1−L5a−k)]BAr_F Catalyst Precursors[a]

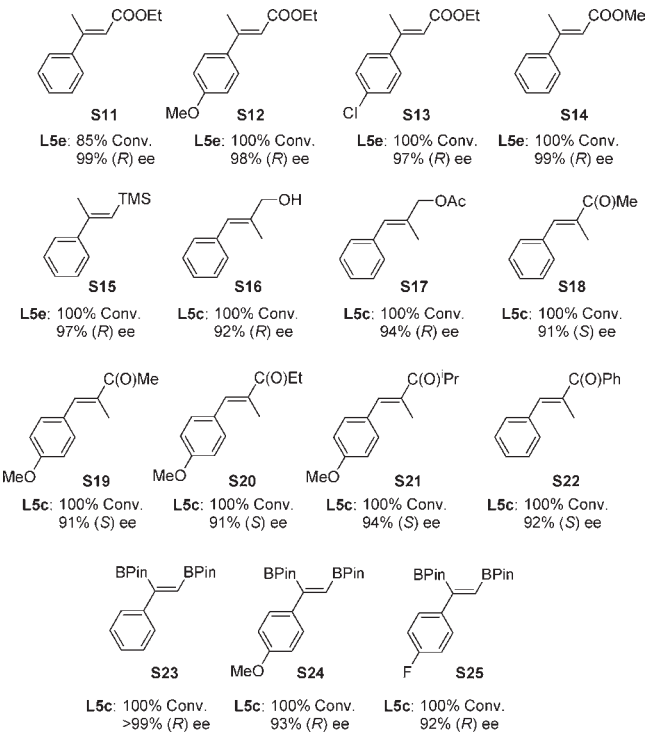

[a] Reaction conditions: 1 mol % catalyst precursor, CH_2Cl_2 as solvent, 50 bar H_2, 2 h.

S16, allylic acetate **S17**, several α,β-unsaturated ketones **S18**−**S22**, and vinylboronates **S23**−**S25**, enantioselectivities were best with ligand **L5c**. It should be pointed out the unprecedented excellent enantioselectivities obtained in the hydrogenation of vinylboronates (ee's ranging from 92% to >99%). The hydrogenation of vinylboronates provides an easy access to chiral borane compounds, which are useful building blocks in organic synthesis because the C−B bond can be readily converted to C−O, C−N, and C−C bonds with retention of the chirality. For α,β-unsaturated ketones and vinylboronates, ee's are again highly independent of the electronic properties of the phenyl substrate ring. Moreover, our results indicate that for enones **S18**−**S22** the substituent linked to the ketone functionality has little effect on enantioselectivity. In summary, Ir/**L1**−**L5a**−**k** complexes have therefore emerged as one of the few catalytic systems that can hydrogenate a wide range of minimally functionalized *E*- and *Z*-trisubstituted olefins (including those containing a neighboring polar group) in high activities and enantioselectivities.[4,5]

2.4. Asymmetric Hydrogenation of 1,1-Disubstituted Terminal Olefins. We next screened ligands **L1**−**L5a**−**k** in the asymmetric hydrogenation of more demanding terminal olefins. Enantioselectivity is more difficult to control in these substrates than in trisubstituted olefins. There are two main reasons for this:[2d,e] (a) the two substituents in the substrate can easily exchange positions in the chiral environment formed by the catalysts, thus reversing the face selectivity (Scheme 5a), and (b) the terminal double bond can isomerize to form the more stable internal alkene, which usually leads to the predominant formation of the opposite enantiomer of the hydrogenated product

Scheme 5

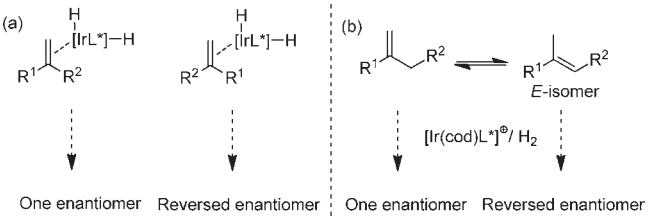

Table 2. Selected Results for the Ir-Catalyzed Hydrogenation of S26 Using the Ligands L1−L5a−k[a]

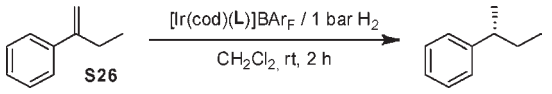

entry	ligand	% conv[b]	% ee[c]
1	**L1c**	100	76 (*S*)
2	**L2c**	100	84 (*S*)
3	**L3c**	100	89 (*S*)
4	**L4c**	100	87 (*S*)
5	**L5a**	99	97 (*S*)
6	**L5b**	<5	–
7	**L5c**	100	92 (*S*)
8	**L5d**	100	97 (*S*)
9	**L5e**	100	99 (*S*)
10	**L5f**	100	39 (*S*)
11	**L5g**	100	94 (*S*)
12	**L5h**	95	34 (*S*)
13	**L5i**	100	97 (*S*)
14	**L5j**	100	23 (*S*)
15	**L5k**	100	98 (*S*)

[a] Reactions carried out using 1 mmol of **S26** and 0.2 mol % of Ir-catalyst precursor at 1 bar of H_2. [b] Conversion measured by GC after 2 h. [c] Enantiomeric excesses determined by chiral GC.

(Scheme 5b). Few known catalytic systems provide high enantioselectivities for these substrates, and those that do are usually limited in substrate scope.[2e,13,14] In contrast to the hydrogenation of trisubstituted olefins, the enantioselectivity in the reduction of terminal alkenes is highly pressure dependent. Therefore, hydrogenation at an atmospheric pressure of H_2 gave, in general, significantly higher ee values than at higher pressures.[4b,13]

2.4.1. Asymmetric Hydrogenation of Unfunctionalized 1, 1-Disubstituted Terminal Olefins. In a first set of experiments, we used the Ir-catalyzed asymmetric hydrogenation of 2-phenylbut-1-ene **S26**. The results obtained using the ligand library **L1**−**L5a**−**k** in optimized conditions are shown in Table 2. We were again able to fine-tune the ligand parameters to produce high activities and enantioselectivities (ee's up to 99%) in the hydrogenation of this substrate using low catalyst loadings (0.2 mol %) and hydrogen pressures (1 bar). Enantioselectivities were affected by the electronic and steric properties of the oxazoline moiety and by the substituents/configurations of the biaryl phosphite group. In general, the effect of these ligand parameters on enantioselectivity followed the same trend as for

Table 3. Selected Results for the Ir-Catalyzed Hydrogenation of Minimally Functionalized 1,1-Disubstituted Terminal Olefins Using Ligands L1−L5a−k[a]

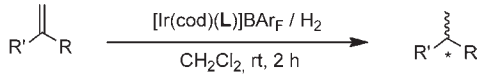

Entry	Substrate	Ligand	% Conv[b]	% ee[c]	Entry	Substrate	Ligand	% Conv[b]	% ee[c]
1	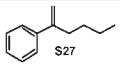 S27	**L5e**	100	90 (*S*)	8	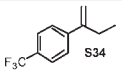 S34	**L5e**	100	99 (*S*)
2	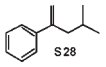 S28	**L5e**	100	93 (*S*)	9	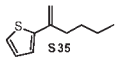 S35	**L5e**	100	90 (-)
3	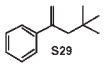 S29	**L5e**	100	93 (*S*)	10	S36	**L5e**	100	99 (+)
4	S30	**L5e**	100	83 (*S*)	11	S37	**L5e**	100	99 (+)
5	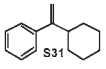 S31	**L5e**	100	84 (*S*)	12[d]	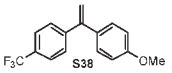 S38	**L5k**	100	65 (+)
6	S32	**L5e**	100	97 (*S*)	13[d]	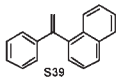 S39	**L5k**	100	70 (+)
7	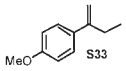 S33	**L5e**	100	98 (*S*)	14[d]	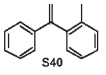 S40	**L5k**	100	68 (+)

[a] Reactions carried out using 1 mmol of substrate and 0.2 mol% of Ir-catalyst precursor at 1 bar of H_2. [b] Conversion measured by ^{1}H-NMR or GC. [c] Enantiomeric excesses determined by chiral GC (except for entries 12-14 that were measured by HPLC). [d] Reaction carried out at 50 bar of H_2.

[a] Reactions carried out using 1 mmol of substrate and 0.2 mol % of Ir-catalyst precursor at 1 bar of H_2. [b] Conversion measured by ^{1}H NMR or GC. [c] Enantiomeric excesses determined by chiral GC (except for entries 12−14 that were measured by HPLC). [d] Reaction carried out at 50 bar of H_2.

the reduction of trisubstituted olefins. However, the effect of the substituents at the *para* positions of the biaryl phosphite moiety is different. Therefore, in contrast to the previous trisubstituted olefins, enantioselectivities increased if the steric bulk of the substituent at the *para* position of the biaryl phosphite moiety decreased (i.e., **L5e** (H)> **L5d** (OMe) > **L5c** (^{t}Bu)). In summary, enantioselectivities were best (99% ee) when phosphite−oxazoline ligand **L5e**, which contains a phenyl group in the oxazoline moiety and bulky *ortho* trimethylsilyl groups at the biphenyl phosphite moiety, was used. This result, which again clearly shows the efficiency of using modular scaffolds in ligand design, is among the best that have been reported for this demanding substrate.[2e]

We then studied the asymmetric hydrogenation of other 1, 1-disubstituted aryl−alkyl substrates (**S27**−**S34**), 1,1-disubstituted heteroaryl−alkyl olefins (**S35**−**S37**), and 1,1-diaryl terminal alkenes (**S38**−**S40**) by using the phosphite−oxazoline ligand library **L1**−**L5a**−**k**. The most noteworthy results are shown in Table 3. Again, these results are among the best reported for these substrates.[2e] For aryl−alkyl and heteroaryl−alkyl substrates (**S27**−**S37**), the results follow the same trends as the hydrogenation of **S26**. Again, the catalyst precursor containing the phosphite−oxazoline ligand **L5e** provided the best enantioselectivities (ee's up to 99%). However, for the hydrogenation of the diaryl terminal alkenes, enantioselectivities were best using ligand **L5k**, which differs from **L5e** in the biaryl phosphite group.

Our results with several 1,1-disubstituted aryl−alkyl substrates (**S26**−**S32**) indicated that enantioselectivity is affected by the nature of the alkyl chain (ee's ranging from 83% to 99%, Table 2, entry 9 and Table 3, entries 1−6). One plausible explanation for this can be found in the competition between direct hydrogenation versus isomerization for the different substrates. This is supported by the fact that the hydrogenation of substrate **S32** bearing a *tert*-butyl group, for which isomerization cannot occur, provides high levels of enantioselectivity (ee's up to 97%; Table 3, entry 6), while the lowest enantioselectivity of the series (ee's up to 84%; Table 3, entries 4,5) is found for substrates **S30** and **S31**, which form the most stable isomerized tetrasubstituted olefins.

The hydrogenations of several *para*-substituted 2-phenylbut-2-enes with different electronic properties (**S26**, **S33**, and **S34**) all gave similar high activities and enantioselectivities (full conversion, ee's up to 99%; Table 2, entry 9 and Table 3, entries 7 and 8).

We next decided to apply this ligand library in the asymmetric hydrogenation of 1,1-heteroaromatic alkenes (**S35**−**S37**, Table 3, entries 9−11). Even though heterocycles are used in industry and the heterocyclic part can be modified posthydrogenation, very few previous studies have been made.[5c,d] Under standard conditions, our catalyst systems were also able to

hydrogenate this type of substrate with excellent activities and enantioselectivities (ee's up to 99%).

Encouraged by the excellent results, we decided to study the hydrogenation of several diaryl terminal alkenes (**S38**−**S40**; Table 3, entries 12−14). Enantiopure diarylalkanes are important intermediates for the preparation of drugs and research materials.[15] They have traditionally been prepared using rather laborious approaches.[15,16] We have recently demonstrated that they can be prepared more efficiently using enantioselective hydrogenation.[5c] Interestingly, both substrate types differing electronically (**S38**) and sterically (**S39**, **S40**) were hydrogenated with fair enantioselectivities (ee's up to 70%) using ligand **L5k**.

2.4.2. Asymmetric Hydrogenation of 1,1-Disubstituted Terminal Olefins Containing a Neighboring Polar Group. To further determine the scope of this ligand library, we also examined the asymmetric hydrogenation of 1,1-disubstituted terminal olefins containing a polar neighboring group (**S41**−**S44**). The results are summarized in Scheme 6.

We initially tested the ligand library in the hydrogenation of the allylic alcohol **S41** and allylic acetate **S42**. Derivatives of the hydrogenation of these products are important intermediates for the synthesis of high-value cosmetics, natural products, and drugs.[17] Enantioselectivities up to 70% were obtained using ligand **L5c**. We then turned our attention to the asymmetric reduction of the trifluoromethyl olefin **S43** and allylic silane **S44**. The hydrogenation of these compounds gave rise to important organic intermediates, and a number of innovative new organofluorine[18] and organosilicon[19] drugs are now being developed. Despite this, only one family of ligands has been successfully applied in the reduction of these substrates.[5c] The enantioselectivities (71% ee for **S43** and 96% ee for **S44**) were best with ligands **L5k** and **L3c**, respectively. These results, which again clearly show the efficiency of using modular scaffolds in ligand design, are among the best that have been reported for these demanding substrate classes.[2e]

Scheme 6. Selected Hydrogenation Results of 1,1-Disubstituted Terminal Olefins Containing a Neighboring Polar Group Using [Ir(cod)(L1−L5a−k)]BAr_F Catalyst Precursors[a]

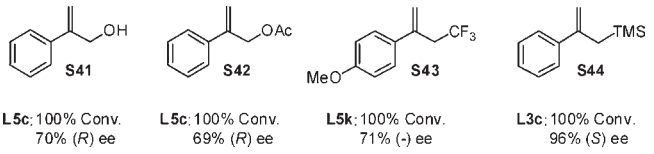

[a] Reaction conditions: 0.5 mol % catalyst precursor, CH_2Cl_2 as solvent, 50 bar H_2, 2 h.

2.5. Origin of Enantioselectivity. Computational Studies. Although the mechanism of olefin hydrogenation (and consequently of stereocontrol) by Rh catalysts is well understood,[20] the mechanism when chiral iridium catalysts are used is not, despite having been investigated both experimentally and computationally.[1,2] In the first case, there is enough evidence to support a Rh^{I}/Rh^{III} mechanism in which substrate chelation to metal plays a pivotal role in stereodiscrimination, but in the second four different mechanisms have been proposed (two of them involving Ir^{I}/Ir^{III} intermediates[21] and the other two Ir^{III}/Ir^{V} species[22]). Andersson and co-workers have recently used DFT calculations and a full, experimentally tested combination of ligands (mainly phosphine/phosphinite,N) and substrates to study all of the possible diastereomeric routes of the four different mechanisms.[23] Their studies agree with the two already proposed catalytic cycles passing through Ir^{III}/Ir^{V} intermediates;[22] however, they failed to distinguish the two Ir^{III}/Ir^{V} mechanisms.[24] One of the mechanisms involves an Ir^{III}/Ir^{V} migratory-insertion/reductive-elimination pathway (labeled 3/5-MI in Scheme 7),[22c] whereas the second mechanism goes through an Ir^{III}/Ir^{V} σ-metathesis/reductive-elimination pathway (labeled 3/5-Meta in Scheme 7).[22a,b] From these cycles, it has been demonstrated that the π-olefin complex **C** and the transition states for the migratory-insertion in 3/5-MI (**TS**) and the σ-metathesis in 3/5-Meta (**TS′**) are responsible for the enantiocontrol in the iridium hydrogenation.[23] It was demonstrated that the enantioselectivity could be reliably obtained from calculated relative energies of migratory insertion transition states.[23]

On the basis of these previous studies and in an attempt to rationalize the enantioselectivity obtained with the iridium/phosphite−oxazoline catalyst library reported in this Article, we performed a computational study of the complexes **C** and transition states (**TS** and **TS′**) most commonly involved in the enantiocontrol of the iridium-catalyzed hydrogenation reaction (Scheme 7).

All geometries were optimized in the gas phase using the Jaguar program[25] and both the B3LYP hybrid density functional[26] and the LACVP* basis set. Termochemical data were computed at 298.15 K for all optimized geometries. Energies in CH_2Cl_2

Scheme 7. 3/5-MI and 3/5-Meta Catalytic Cycles for the Ir-Hydrogenation

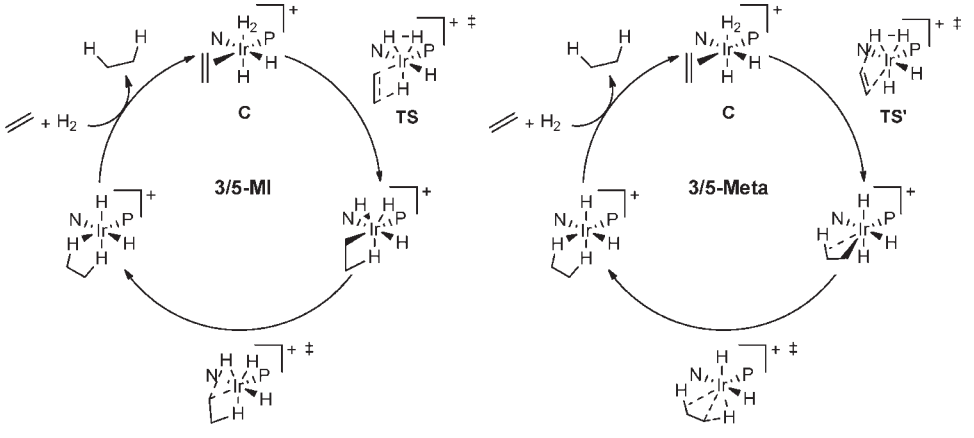

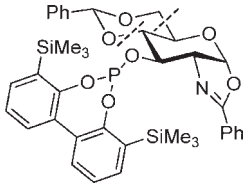

Figure 2. Ligand truncation used for preliminary DFT calculations.

Table 4. Calculated Energies for the Most Stable Isomers of Complex C and Transition States TS and TS′ with Substrate S1 Using the Truncated Ligand System

3/5-MI cycle			3/5-Meta cycle		
Starting geometry	C energy (kJ/mol)	TS energy (kJ/mol)	Starting geometry	C energy (kJ/mol)	TS' energy (kJ/mol)
$C1_{3/5\text{-MI}}$	-45.6	0 (ref)	$C1_{3/5\text{-Meta}}$	-41.2	20.2
$C2_{3/5\text{-MI}}$	-47.4	51.6	$C2_{3/5\text{-Meta}}$	-47.2	26.5
$C3_{3/5\text{-MI}}$	-32.5	15.6	$C3_{3/5\text{-Meta}}$	-47.9	64.0
$C4_{3/5\text{-MI}}$	-28.3	61.5	$C4_{3/5\text{-Meta}}$	-59.4	27.9

solution were calculated as single-point energies from optimized structures at the B3LYP/LACVP* level of theory using a Poisson−Boltzmann continuous field. Final energies were retrieved from single-point calculations at the B3LYP/LACV3P++* level of theory and corrected by inclusion of the van der Waals repulsion energy calculated by DFT-D3.[27] Reported energies (in kJ/mol) are the Gibbs free energy, including thermodynamic and solvation contributions. For more computational details, see the Experimental Section and the Supporting Information.

This computational study has been performed with two different types of substrate: **S1** as a model substrate for trisubstituted olefins and **S26** as a model for 1,1-disubstituted olefins. We chose to study the catalyst precursor Ir/**L5e** because for both substrates **L5e** proved to have the best combination of ligand parameters for high enantioselectivity. For preliminary calculations, the ligand was simplified by removing the benzylidene protecting group (Figure 2) in an attempt to accelerate the DFT calculation and verify whether the method gave satisfactory results. The method then was used to explore the reactions involving the complete ligand.

Initially, we applied the calculation for the trisubstituted olefin **S1**. Both 3/5-MI and 3/5-Meta mechanisms were investigated for all approach vectors of the alkene. Table 4 shows the calculated energies for the most stable isomers of complex **C** and for the most stable isomers of the transition states (**TS** and **TS′**) with the truncated ligand. These key isomers are the result of varying the relative coordination of the substrate (*si* face or *re* face) and the relative position of the hydride (up or down).[28] The olefins coordinated on the *si* face are shown in green and are hydrogenated to (*R*)-product, whereas those coordinated on the *re* face are shown in red and are hydrogenated to the (*S*)-product. The results show that the most stable transition state ($C1_{3/5\text{-MI}}$, Table 4) matches the major product obtained experimentally (*R* product, Table 1, entry 9). We also found that the hydrogenation products are formed through the 3/5-MI mechanism, with the best 3/5-Meta path significantly higher in energy for both enantiomers. Therefore, the energies for hydrogenation pathway 3/5-MI, in both the major and the minor configurations, are around 15 kJ/mol more stable than those for the 3/5-Meta pathway (see Table 4). In addition, the difference in energy between the most stable transition state for the major and the minor product is 15.6 kJ/mol, which agrees with the excellent enantioselectivity obtained experimentally using the Ir/**L5e** catalyst system (Table 1, entry 9).

Because the method gives satisfactory results, we next applied it to the reaction of **S1** with the full ligand structure. The difference in energy of 22.9 kJ/mol between the most stable transition states (Figure 3) matches well with the excellent enantioselectivities obtained experimentally (>99% ee, Table 1, entry 9).

The optimized DFT structure shows a quadrant diagram (depicted in Figure 4), a model already used by Andersson and co-workers to describe the steroselectivity in the Ir-catalyzed hydrogenation of trisubstituted olefins.[4d] In this quadrant model, we found that the phenyl group of the oxazoline substituent blocks the upper left quadrant, and one of the aryls of the biaryl phosphite group partly occupies the lower right quadrant making it semihindered (Figure 4a). The other two quadrants, which are free from bulky groups, are open (Figure 4a). Therefore, the calculated structure clearly shows a chiral pocket that is well suited to olefins with large *trans*-substituents (*E*-olefins). In the case of the trisubstituted *E*-olefin **S1**, the smallest substituent (H atom of **S1**) will face the steric bulk of the ligand, and the olefin will preferentially coordinate to the catalyst from the *si* side (Figure 4b), as the opposite coordination mode will result in unfavorable interactions between one of the large *trans*-substituents and the steric bulk of the ligand.

This model also explains the lack of enantioselectivity observed when ligands **L5f**, **L5h**, and **L5j** were used (Table 1, entries 10, 12, and 14). In all tof hese ligands, the biaryl phosphite group has an *S*-configuration, which is opposite to the configuration adopted by ligand **L5e** when coordinated to the Ir, as shown by the catalytic results and the DFT calculation (Figures 3 and 4a). This change in the configuration moves the previously found semihindered quadrant from the lower right to the upper right. Therefore, the favorable chiral pocket generated by the Ir/**L5e** catalyst, which can accommodate large *trans*-substituents, is lost, and consequently Ir/**L5f**, Ir/**L5h**, and Ir/**L5j** catalysts fail to control the face coordination preference of the olefin.

Using this quadrant model, we can also predict the change in the sense of enantioselectivity observed experimentally when *E*-trisubstituted olefins (i.e., **S1**) change to *Z*-olefins (i.e., **S2**). The lowest energy transition state, then, will be achieved with the *Z*-olefin coordinated through the *re* face, the opposite face to that of the *E*-olefin, with the hydrogen atom positioned in the hindered upper left quadrant and the aryl substituent in the semihindered lower right quadrant (Figure 4c). The catalytic results also show that to obtain high enantioselectivity in the reduction of *Z*-olefins we have to switch to ligand **L5c**. This is not unexpected because the DFT calculations have shown that the catalytic system Ir/**L5e**

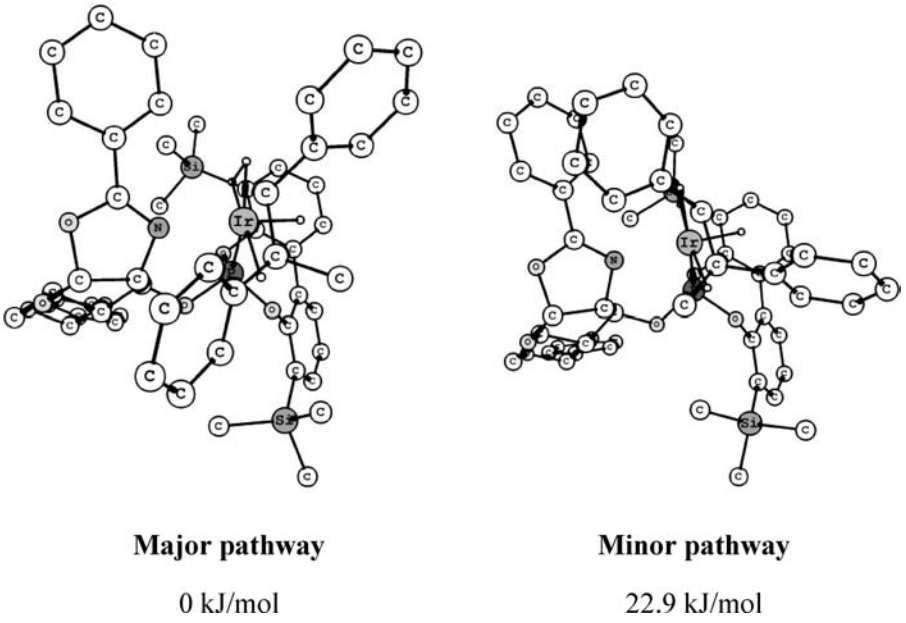

Figure 3. Calculated transition states (TS) for the major and the minor pathways with the full ligand. Hydrogen atoms of the ligand **L5e** and substrate **S1** have been omitted for clarity.

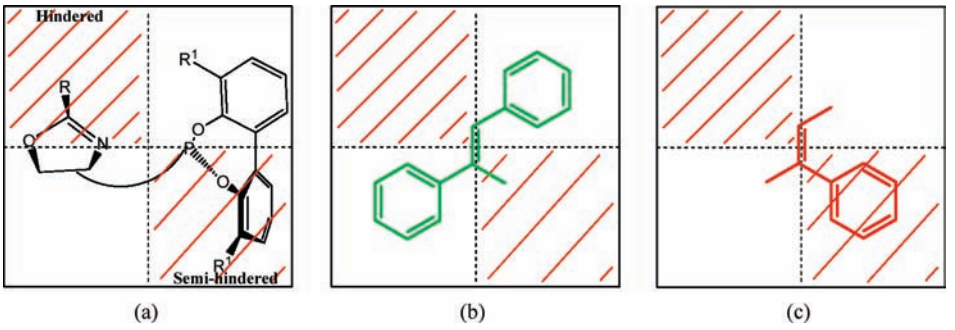

Figure 4. Quadrant diagram describing the enantioselective substrate−ligand interactions.

generated a pocket that is well suited to *E*-olefins. Ligand **L5c** differs from the previous ligand **L5e** in the presence of bulky substituents at the *para* position of the biphenyl group. These substituents increase the dihedral angle of the biaryl group, which results in lower occupancy of the lower right quadrant than with the previous Ir/**L5e** catalytic system. So, the substituents of the biphenyl moieties can tune the steric hindrance of the lower right quadrant so that it can accommodate the phenyl substituent of *Z*-substrates and lead to high enantioselectivity. The same explanation may account for the excellent enantioselectivities obtained with triarylsubstituted olefins **S9** and **S10**.

Finally, we did the calculation for the 1,1-disubstituted olefin **S26**, using first the truncated ligand structure of **L5e** without the benzylidene protecting group (Figure 2). We found that the results followed the same trend as for the trisubstituted olefin (Table 5). Therefore, the most stable transition state observed matches the major product, and the preferred pathway is the 3/5-MI with an energy difference of 15 kJ/mol with respect to the 3/5-Meta pathway. Using the full structure of ligand **L5e**, we observe that the difference in energy between the transition states for the major and the minor products is 9.5 kJ/mol (Figure 5). Thus, not only is the major isomer correctly identified for this challenging system, but the quantitative prediction of 96% ee at ambient temperature matches well with the enantioselectivity obtained experimentally (99% ee, Table 2, entry 9).

In summary, the substrate versatility of our Ir/phosphite−oxazoline catalytic system is higher than that of related Ir−phosphine/phosphinite−nitrogen catalysts because the biaryl phosphite moiety makes the catalyst more flexible. Therefore, subtle variations in the dihedral angle of the biaryl phosphite moiety, which may arise from changing the biaryl substituents and/or be imposed by the substrate itself, lead to a different occupancy of the semihindered quadrant. As a result, the catalyst can adapt its chiral environment to a range of substrate types.

3. CONCLUSIONS

The modular ligand design has been shown to be highly successful, both in finding highly selective ligands for each substrate and in identifying two general ligands (**L5c** and **L5e**) with good performance over the entire range of substrates. The good performance extends even to the very challenging class of terminally disubstituted olefins. The enantioselectivity was below 90% for olefins with two similarly sized substituents, such as aryl

versus aryl or *s*-alkyl, but even a moderate size difference like aryl versus *n*-alkyl allowed good enantioselectivities in the range 90−99%. It should be pointed out that these catalysts are also very tolerant to the presence of neighboring polar group. Thus, a range of allylic alcohols, acetates, α,β-unsaturated ketones, α,β-unsaturated esters, and vinylboronates were hydrogenated in high enantioselectivities (ee's up to >99%).

The computational study allowed identification of the preferred reaction path, an Ir(III/V) cycle with migratory insertion of a hydride as the selectivity-determining step.[23] The alternative metathesis mechanism[22a,b] was consistently higher in energy. For selected models, the DFT calculations allowed computational determination of the observed selectivities with high accuracy.

Table 5. Calculated Energies for the Most Stable Isomers of Complex C and Transition States TS and TS′ with Substrate S26 Using the Truncated Ligand System

3/5-MI cycle			3/5-Meta cycle		
Starting geometry	C energy (kJ/mol)	TS energy (kJ/mol)	Starting geometry	C energy (kJ/mol)	TS' energy (kJ/mol)
$C5_{3/5\text{-MI}}$	-45.0	0 (ref)	$C5_{3/5\text{-Meta}}$	-36.1	20.1
$C6_{3/5\text{-MI}}$	-44.0	7.4	$C6_{3/5\text{-Meta}}$	-40.9	21.9
$C7_{3/5\text{-MI}}$	-40.3	11.4	$C7_{3/5\text{-Meta}}$	-41.4	27.6
$C8_{3/5\text{-MI}}$	-39.5	59.2	$C8_{3/5\text{-Meta}}$	-38.0	40.9

Both the favored enantiomer and the effect of ligand modifications could be rationalized in terms of the previously proposed quadrant model.

4. EXPERIMENTAL SECTION

4.1. General Considerations. All reactions were carried out using standard Schlenk techniques under an argon atmosphere. Solvents were purified and dried by standard procedures. Phosphorochloridites are easily prepared in one step from the corresponding biaryls.[29] Ligands **L1**−**L3c**, **L5a**−**e**, and **L5h**−**k** were prepared as previously described.[5a,7] [Ir(cod)(L)]BArF (L = **L1**−**L3c**, **L5c**−**e**, **L5h,i**, and **L5k**) were prepared previously.[5a] ^{1}H, $^{13}C\{^{1}H\}$, and $^{31}P\{^{1}H\}$ NMR spectra were recorded using a 400 MHz spectrometer. Chemical shifts are relative to that of $SiMe_4$ (^{1}H and ^{13}C) as internal standard or H_3PO_4 (^{31}P) as external standard. ^{1}H, ^{13}C, and ^{31}P assignments were made on the basis of $^{1}H-^{1}H$ gCOSY, $^{1}H-^{13}C$ gHSQC, and $^{1}H-^{31}P$ gHMBC experiments. All catalytic experiments were performed three times.

4.2. Computational Details. Geometries of all substrates were optimized using the Jaguar program[25] and both the B3LYP hybrid density functional[26] and the LACVP* basis sets. The complexes were treated with charge = +1 and in the singlet state. In some cases, structures were first optimized using geometric constraints to generate starting structures that were subsequently optimized without geometric constraints. No symmetry constraints were applied. Normal-mode analysis of stable structure revealed no imaginary frequencies or a single imaginary frequency with negligibly low frequency ($\nu < 100$ cm^{-1}); those of transition states had a single imaginary frequency of higher negative frequency (usually $\nu < -500$ cm^{-1}). Reported energies are the Gibbs free energy at 298.15 K. LACVP in Jaguar defines a combination of the LANL2DZ basis set[30] for iridium and the 6-31G basis set for other atoms. Final energies were retrieved from single-point calculations at the B3LYP/LACV3P++* level of theory. LACV3P++* differs from LACVP* because it uses the 6-311++G* basis set instead of 6-31G*, one additional p function, and two additional d functions on Ir. Energies in CH_2Cl_2 solution were calculated as single-point energies from optimized

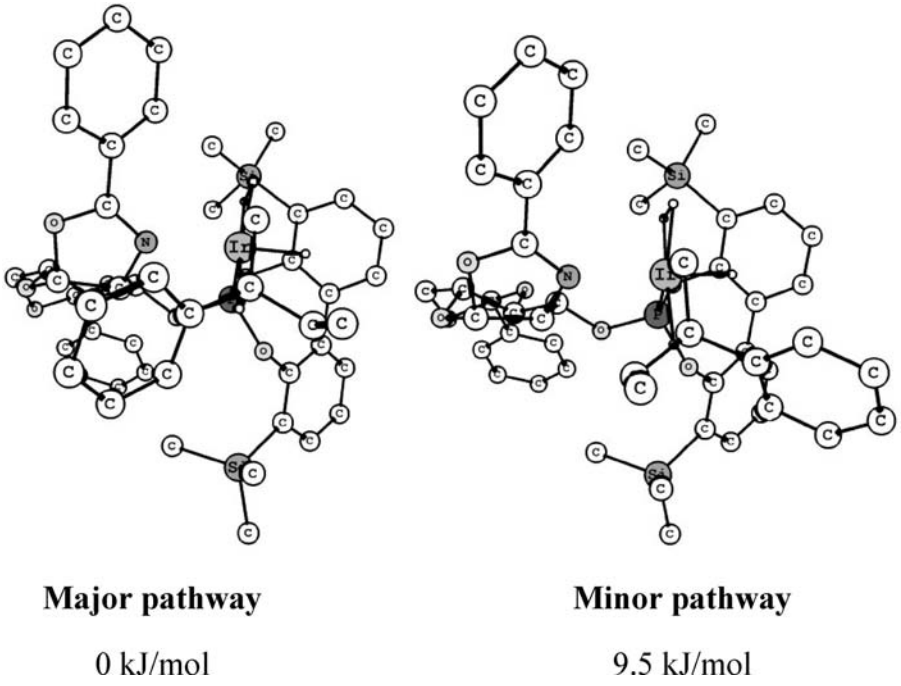

Figure 5. Calculated transitions states (TS) for the major and the minor pathways with the full ligand. Hydrogen atoms of the ligand **L5e** and substrate **S26** have been omitted for clarity.

structures at the B3LYP/LACVP* level of theory using a Poisson−Boltzmann continuous field with ε = 8.93 and F = 1.3266 g/mL to calculate the solvent radius (2.33 Å).[31] Final energies were corrected by inclusion of the van der Waals repulsion energy calculated by DFT-D3.[27]

4.3. General Procedure for the Preparation of the Phosphite−Oxazoline Ligands. The corresponding phosphorochloridite (3.0 mmol) produced in situ was dissolved in toluene (12.5 mL), and pyridine (1.14 mL, 14 mmol) was added. The corresponding hydroxyl−oxazoline compound (2.8 mmol) was azeotropically dried with toluene (3 × 2 mL) and then dissolved in toluene (12.5 mL) to which pyridine (1.14 mL, 14 mmol) was added. The oxazoline solution was transferred slowly at 0 °C to the solution of phosphorochloridite. The reaction mixture was stirred overnight at 80 °C, and the pyridine salts were removed by filtration. Evaporation of the solvent gave a white foam, which was purified by flash chromatography in alumina to produce the corresponding ligand as a white solid.

L5f. Yield: 1.0 g (48%). ^{31}P NMR ($CDCl_3$), δ: 147.3 (s). ^{1}H NMR (C_6D_6), δ: 1.44 (s, 9H, CH_3, ^{t}Bu), 1.69 (s, 9H, CH_3, ^{t}Bu), 1.74 (s, 3H, CH_3−Ar), 1.81 (s, 3H, CH_3−Ar), 2.09 (s, 3H, CH_3−Ar), 2.11 (s, 3H, CH_3−Ar), 3.52 (m, 1H, H-6′), 3.67 (m, 1H, H-5), 3.78 (m, 1H, H-4), 4.11 (m, 1H, H-2), 4.27 (m, 1H, H-6), 4.92 (m, 1H, H-3), 5.52 (d, 1H, H-1, $^3J_{1-2}$= 7.6 Hz), 5.57 (s, 1H, H-7), 7.14−7.83 (m, 12H, CH═). ^{13}C NMR (C_6D_6), δ: 16.1 (CH_3−Ar), 16.4 (CH_3−Ar), 19.8 (CH_3−Ar), 20.0 (CH_3−Ar), 32.9 (CH_3, ^{t}Bu), 33.1 (CH_3, ^{t}Bu), 35.9 (C, ^{t}Bu), 36.0 (C, ^{t}Bu), 64.5 (C-5), 70.3 (C-6), 70.5 (C-2), 79.1 (C-3), 81.0 (C-4), 102.9.0 (C-7), 103.2 (C-1), 125.7 (CH═), 125.8 (CH═), 127.0 (CH═), 128,1 (CH═), 128.4 (CH═), 128.6 (CH═), 129.1 (CH═), 129.4 (CH═), 129,6 (CH═), 129.7 (CH═), 129.9 (CH═), 130.4 (CH═), 130.7 (CH═), 130.9 (C), 131.8 (C), 132.1 (C), 132.2 (C), 132.5 (C), 134.4 (C), 135.2 (C), 137.3 (C), 137.6 (C), 138.0 (C), 144.6 (C), 145.3 (C), 165.7 (C═N). Anal. Calcd for $C_{44}H_{50}NO_7P$: C, 71.82; H, 6.85; N, 1.90. Found: C, 71.87; H, 6.93; N, 1.88.

L5g. Yield: 1.1 g (52%). ^{31}P NMR ($CDCl_3$), δ: 147.8 (s). ^{1}H NMR (C_6D_6), δ: 1.43 (s, 9H, CH_3, ^{t}Bu), 1.63 (s, 9H, CH_3, ^{t}Bu), 1.71 (s, 3H, CH_3−Ar), 1.83 (s, 3H, CH_3−Ar), 2.11 (s, 6H, CH_3−Ar), 3.53 (m, 1H, H-6′), 3.68 (m, 1H, H-5), 3.73 (m, 1H, H-4), 4.14 (m, 1H, H-2), 4.25 (m, 1H, H-6), 4.75 (m, 1H, H-3), 5.51 (d, 1H, H-1, $^3J_{1-2}$= 7.6 Hz), 5.58 (s, 1H, H-7), 7.14−7.83 (m, 12H, CH═). ^{13}C NMR (C_6D_6), δ: 16.1 (CH_3−Ar), 16.4 (CH_3−Ar), 19.9 (CH_3−Ar), 33.1 (CH_3, ^{t}Bu), 35.9 (C, ^{t}Bu), 36.0 (C, ^{t}Bu), 64.6 (C-5), 70.2 (C-6), 71.2 (C-2), 79.8 (C-3), 80.5 (C-4), 102.9 (C-7), 103.1 (C-1), 125.8 (CH═), 125.9 (CH═), 126.8 (CH═), 128,0 (CH═), 128.6 (CH═), 128.9 (CH═), 129.5 (CH═), 129.7 (CH═), 129.8 (CH═), 130.7 (CH═), 130.9 (CH═), 131.7 (CH═), 131.9 (C), 132.3 (C), 132.5 (C), 132.8 (C), 134.5 (C), 135.2 (C), 137.3 (C), 137.6 (C), 138.0 (C), 144.6 (C), 145.3 (C), 165.9 (C═N). Anal. Calcd for $C_{44}H_{50}NO_7P$: C, 71.82; H, 6.85; N, 1.90. Found: C, 71.85; H, 6.89; N, 1.89.

4.4. Typical Procedure for the Preparation of [Ir(cod)(L)]BAr$_F$. The corresponding ligand (0.074 mmol) was dissolved in CH_2Cl_2 (2 mL), and [Ir(μ-Cl)cod]$_2$ (25 mg, 0.037 mmol) was added. The reaction was refluxed at 50 °C for 1 h. After 5 min at room temperature, $NaBAr_F$ (77.1 mg, 0.082 mmol) and water (2 mL) were added, and the reaction mixture was stirred vigorously for 30 min at room temperature. The phases were separated, and the aqueous phase was extracted twice with CH_2Cl_2. The combined organic phases were filtered through a Celite plug, dried with $MgSO_4$, and the solvent was evaporated to give the product as an orange solid.

*[Ir(cod)(**L4c**)]BAr$_F$*. Yield: 138 mg (95%). ^{31}P NMR ($CDCl_3$), δ: 104.3 (s). ^{1}H NMR ($CDCl_3$), δ: 1.36 (s, 9H, CH_3, ^{t}Bu), 1.41 (s, 9H, CH_3, ^{t}Bu), 1.65 (s, 2H, CH_2), 1.70 (s, 9H, CH_3, ^{t}Bu), 1.73 (s, 9H, CH_3, ^{t}Bu), 1.8−2.2 (b, 8H, CH_2, cod), 3.48 (m, 1H, H-6′), 3.65 (m, 2H, CH═, cod and H-5), 3.84 (m, 1H, H-4), 4.13 (m, 1H, H-2), 4.15 (b, 1H, CH═, cod), 4.24 (dd, 1H, H-6, $^2J_{6-6'}$ = 10.0 Hz, $^3J_{6-5}$ = 4.8 Hz), 4.79 (b, 1H, CH═, cod), 4.92 (m, 1H, H-3), 5.18 (b, 1H, CH═, cod), 5.49 (d, 1H, H-1, $^3J_{1-2}$= 7.6 Hz), 5.53 (s, 1H, H-7), 7.1−8.5 (m, 26H, CH═, aromatics). ^{13}C NMR ($CDCl_3$), δ: 15.3 (CH_2), 22.8 (b, CH_2, cod), 28.9 (b, CH_2, cod), 31.3 (CH_3, ^{t}Bu), 31.4 (CH_3, ^{t}Bu), 31.6 (CH_3, ^{t}Bu), 32.4 (b, CH_2, cod), 32.9 (b, CH_2, cod), 34.9 (C, ^{t}Bu), 35.1 (C, ^{t}Bu), 35.5 (C, ^{t}Bu), 36.0 (C, ^{t}Bu), 64.7 (C-5), 67.1 (CH═, cod), 70.4 (C-2), 70.7 (C-6), 72.3 (CH═, cod), 79.5 (d, C-3, $^2J_{C-P}$ = 20.5 Hz), 80.3 (C-4), 99.6 (b, CH═, cod), 103.0 (C-7), 103.2 (C-1), 104.1 (d, CH═, cod, J_{C-P} = 12.2 Hz), 117.7 (b, CH═, BAr_F), 119−134 (aromatic carbons), 135.0 (b, CH═, BAr_F), 136−149 (aromatic carbons), 161.9 (q, C−B, BAr_F, $^1J_{C-B}$ = 49.6 Hz), 168.7 (C═N). Anal. Calcd for $C_{89}H_{84}BF_{24}IrNO_7P$: C, 54.27; H, 4.30; N, 0.71. Found: C, 54.32; H, 4.35; N, 0.68.

*[Ir(cod)(**L5a**)]BAr$_F$*. Yield: 118 mg (92%). ^{31}P ($CDCl_3$), δ: 112.7 (s). ^{1}H ($CDCl_3$), δ: 1.7−2.4 (b, 8H, CH_2, cod), 3.73 (m, 2H, H-5, H-6′), 3.81 (m, 2H, CH═, cod and H-4), 4.24 (b, 1H, CH═, cod), 4.41 (m, 2H, H-6, H-2), 4.71 (b, 1H, CH═, cod), 4.77 (m, 1H, H-3), 5.33 (b, 1H, CH═, cod), 5.69 (s, 1H, H-7), 6.03 (d, 1H, H-1, $^3J_{1,2}$ = 7.2 Hz), 7.1−8.2 (m, 30H, CH═). ^{13}C ($CDCl_3$), δ: 22.4 (b, CH_2, cod), 23.1 (b, CH_2, cod), 31.9 (b, CH_2, cod), 32.3 (b, CH_2, cod), 63.2 (C-5), 68.9 (C-6), 70.2 (C-2), 76.7 (C-3), 80.0 (C-4), 100.5 (d, CH═, cod, J_{C-P} = 18 Hz), 101.6 (C-7), 102.7 (C-1), 103.3 (d, CH═, cod, J_{C-P} = 22 Hz), 117.8 (b, CH═, BAr_F), 119−134 (aromatic carbons), 135.1 (b, CH═, BAr_F), 136−149 (aromatic carbons), 161.7 (q, C−B, BAr_F, $^1J_{C-B}$ = 49.6 Hz), 170.3 (C═N). Anal. Calcd for $C_{72}H_{50}BF_{24}IrNO_7P$: C, 49.95; H, 2.91; N, 0.81. Found: C, 50.02; H, 2.93; N, 0.79.

*[Ir(cod)(**L5b**)]BAr$_F$*. Yield: 134 mg (93%). ^{31}P NMR ($CDCl_3$), δ: 113.5 (s). ^{1}H NMR ($CDCl_3$), δ: 1.8−2.1 (b, 6H, CH_2, cod), 2.19 (s, 3H, CH_3), 2.28 (b, 5H, CH_2, cod and CH_3), 2.34 (s, 3H, CH_3), 2.39 (s, 3H, CH_3), 3.54 (m, 2H, CH═, cod and H-6′), 3.63 (m, 1H, H-4), 3.68 (m, 1H, CH═, cod and H-5), 4.21 (m, 1H, H-6), 4.33 (m, 1H, H-2), 4.39 (b, 1H, CH═, cod), 4.81 (m, 1H, H-3), 5.11 (b, 1H, CH═, cod), 5.46 (s, 1H, H-7), 5.71 (d, 1H, H-1, $^2J_{1-2}$ = 7.5 Hz), 7.1−8.5 (m, 26H, aromatics). ^{13}C NMR ($CDCl_3$), δ: 17.2 (CH_3), 17.4 (CH_3), 21.1 (CH_3), 21.3 (CH_3), 23.1 (b, CH_2, cod), 25.4 (b, CH_2, cod), 33.4 (b, CH_2, cod), 33.6 (b, CH_2, cod), 68.9 (C-6), 68.4 (CH═, cod), 69.5 (C-2), 70.5 (CH═, cod), 78.6 (d, C-3, $^2J_{c-p}$ = 12 Hz), 78.4 (C-4), 99.9 (d, CH═, cod, J_{C-P} = 22.2 Hz), 102.1 (C-7), 103.2 (C-1), 104.3 (d, CH═, cod, J_{C-P} = 16 Hz), 117.6 (b, CH═, BAr_F), 119−134 (aromatic carbons), 135.1 (b, CH═, BAr_F), 136−149 (aromatic carbons), 161.6 (q, C−B, BAr_F, $^1J_{C-B}$ = 49.6 Hz), 170.4 (C═N). Anal. Calcd for $C_{76}H_{58}BF_{24}IrNO_7P$: C, 51.07; H, 3.27; N, 0.78. Found: C, 51.11; H, 3.32; N, 0.80.

*[Ir(cod)(**L5f**)]BAr$_F$*. Yield: 134 mg (94%). ^{31}P NMR ($CDCl_3$), δ: 108.4 (s). ^{1}H NMR ($CDCl_3$), δ: 1.41 (s, 9H, CH_3, ^{t}Bu), 1.57 (s, 9H, CH_3, ^{t}Bu), 1.69 (s, 3H, CH_3−Ar), 1.77 (s, 3H, CH_3−Ar), 1.8−2.1 (b, 7H, CH_2, cod and CH_3−Ar), 2.14 (s, 3H, CH_3−Ar), 2.2−2.4 (b, 4H, CH_2, cod), 3.52 (m, 1H, H-6′), 3.65 (m, 1H, CH═, cod), 3.68 (m, 1H, H-5), 3.82 (m, 1H, H-4), 4.08 (b, 2H, CH═, cod and H-2), 4.23(m, 1H, H-6), 4.79 (b, 1H, CH═, cod), 4.83 (m, 1H, H-3), 5.32 (b, 1H, CH═, cod), 5.49 (d, 1H, H-1, $^3J_{1-2}$ = 7.6 Hz), 5.59 (s, 1H, H-7), 7.1−8.3 (m, 24H, aromatics). ^{13}C NMR ($CDCl_3$), δ: 16.1 (CH_3−Ar), 16.4 (CH_3−Ar), 17.8 (CH_3−Ar), 19.1 (CH_3−Ar), 26.8 (b, CH_2, cod), 27.6 (b, CH_2, cod), 31.3 (CH_3, ^{t}Bu), 31.4 (CH_3, ^{t}Bu), 33.7 (b, CH_2, cod), 34.9 (C, ^{t}Bu), 35.1 (C, ^{t}Bu), 64.7 (C-5), 68.8 (CH═, cod), 70.5 (C-2), 71.1 (CH═, cod), 79.2 (C-3), 81.3 (C-4), 100.4 (d, CH═, cod, J_{C-P} = 21.8 Hz), 102.7 (C-7), 103.1 (b, CH═, cod), 103.6 (C-1), 117.4 (b, CH═, BAr_F), 119−134 (aromatic carbons), 135.1 (b, CH═, BAr_F), 136−149 (aromatic carbons), 161.6 (q, C−B, BAr_F, $^1J_{C-B}$ = 49.6 Hz), 169.4 (C═N). Anal. Calcd for $C_{82}H_{74}BF_{24}IrNO_7PSi_2$: C, 50.99; H, 3.86; N, 0.73. Found: C, 51.02; H, 3.92; N, 0.72.

*[Ir(cod)(**L5g**)]BAr$_F$*. Yield: 142 mg (95%). ^{31}P NMR ($CDCl_3$), δ: 107.6 (s). ^{1}H NMR ($CDCl_3$), δ: 1.40 (s, 9H, CH_3, ^{t}Bu), 1.55 (s, 9H, CH_3, ^{t}Bu), 1.78 (s, 3H, CH_3−Ar), 1.81 (s, 3H, CH_3−Ar), 1.8−2.1 (b, 7H, CH_2, cod and CH_3−Ar), 2.2−2.4 (b, 7H, CH_2, cod and CH_3−Ar), 3.57 (m, 2H, H-6′ and CH═, cod), 3.69 (m, 1H, H-5), 3.95 (m, 1H,

H-4), 4.11 (b, 2H, CH═, cod and H-2), 4.19 (m, 1H, H-6), 4.27 (b, 1H, CH═, cod), 4.79 (m, 1H, H-3), 5.28 (b, 1H, CH═, cod), 5.32 (d, 1H, H-1, $^3J_{1-2}$ = 7.6 Hz), 5.57 (s, 1H, H-7), 7.1−8.3 (m, 24H, aromatics). ^{13}C NMR ($CDCl_3$), δ: 16.3 (CH_3−Ar), 16.5 (CH_3−Ar), 18.4 (CH_3−Ar), 18.9 (CH_3−Ar), 27.2 (b, CH_2, cod), 27.4 (b, CH_2, cod), 31.6 (CH_3, ^{t}Bu), 31.9 (CH_3, ^{t}Bu), 32.4 (b, CH_2, cod), 32.8 (b, CH_2, cod), 34.9 (C, ^{t}Bu), 35.1 (C, ^{t}Bu), 64.9 (C-5), 71.3 (CH═, cod), 71.6 (CH═, cod), 71.9 (C-2), 79.4 (C-3), 80.4 (C-4), 100.9 (b, CH═, cod), 102.7 (C-7), 103.3 (b, CH═, cod), 103.7 (C-1), 117.5 (b, CH═, BAr_F), 119−134 (aromatic carbons), 135.1 (b, CH═, BAr_F), 136−149 (aromatic carbons), 161.7 (q, C−B, BAr_F, $^1J_{C-B}$ = 49.6 Hz), 169.1 (C═N). Anal. Calcd for $C_{82}H_{74}BF_{24}IrNO_7PSi_2$: C, 50.99; H, 3.86; N, 0.73. Found: C, 51.09; H, 3.96; N, 0.71.

*[Ir(cod)(**L5i**)]BAr$_F$.* This compound has been prepared following a slight modification of the general procedure.[9] Yield: 115 mg (91%). ^{31}P NMR ($CDCl_3$), δ: 107.7 (s). ^{1}H NMR ($CDCl_3$), δ: 1.6−2.5 (m, 8H, CH_2 cod), 3.85 (b, 3H, CH═, cod, H-5 and H-6′), 3.91 (m, 1H, H-3), 3.98 (b, 2H, CH═, cod and H-4), 4.01 (b, 1H, CH═, cod), 4.33 (m, 1H, H-6), 4.71 (m, 1H, H-2), 4.99 (b, 1H, CH═, cod), 5.45 (s, 1H, H-7), 5.51 (b, 1H, CH═, cod), 6.31 (d, 1H, H-1, $^3J_{1-2}$ = 6.4 Hz), 7.1−8.3 (m, 32H, CH═, aromatics). ^{13}C NMR ($CDCl_3$), δ: 26.3 (b, CH_2, cod), 28.5 (b, CH_2, cod), 32.3 (b, CH_2, cod), 34.5 (b, CH_2, cod), 64.5 (CH═, cod), 65.9 (C-5), 69.8 (C-6), 70.8 (CH═, cod), 70.9 (C-2), 74.3 (C-4), 80.3 (C-3), 98.4 (d, CH═, cod, J_{C-P} = 22 Hz), 101.8 (s, C-7), 102.9 (d, CH═, cod, J_{C-P} = 12.2 Hz), 103.8 (s, C-1), 117.7 (b, CH═, BAr_F), 120−134 (aromatic carbons), 135.0 (b, CH═, BAr_F), 135−137 (aromatic carbons), 161.7 (q, C−B BAr_F, $^1J_{C-B}$ = 49 Hz), 170.3 (s, C═N). Anal. Calcd for $C_{72}H_{52}BF_{24}IrNO_5P$: C, 50.83; H, 3.08; N, 0.82. Found: C, 51.02; H, 3.14; N, 0.80.

4.5. Typical Procedure for the Hydrogenation of Olefins. The alkene (1 mmol) and Ir complex (0.2 mol %) were dissolved in CH_2Cl_2 (2 mL) in a high-pressure autoclave, which was purged four times with hydrogen. Next, it was pressurized at the desired pressure. After the desired reaction time, the autoclave was depressurized and the solvent evaporated off. The residue was dissolved in Et_2O (1.5 mL) and filtered through a short Celite plug. The enantiomeric excess was determined by chiral GC or chiral HPLC, and conversions were determined by ^{1}H NMR. The enantiomeric excesses of hydrogenated products were determined using the conditions previously described.[4d,q,s,5c]

■ ASSOCIATED CONTENT

Supporting Information. All energies (electronic, nuclear repulsion, free energies, ZPE, and DFT-D3 attraction correction) and structures for all complexes and transition states. Full list of catalytic results. This material is available free of charge via the Internet at http://pubs.acs.org.

■ AUTHOR INFORMATION

Corresponding Author
pon@chem.gu.se; pher.andersson@biorg.uu.se; montserrat.dieguez@urv.cat

■ ACKNOWLEDGMENT

We would like to thank the COST D40, the Spanish Government for providing grants Consolider Ingenio Intecat-CSD2006-0003, CTQ2010-15835, 2008PGIR/07 to O.P. and 2008PGIR/08 to M.D., the Catalan Government for grant 2009SGR116, and the ICREA Foundation for providing M.D. and O.P. with financial support through the ICREA Academia awards.

■ REFERENCES

(1) (a) *Asymmetric Catalysis in Industrial Scale: Challenges, Approaches and Solutions*; Blaser, H. U., Schmidt, E., Eds.; Wiley: Weinheim, Germany, 2003. (b) *Catalytic Asymmetric Synthesis*; Ojima, I., Ed.; Wiley-VCH: New York, 2000. (c) Brown, J. M. In *Comprehensive Asymmetric Catalysis*; Jacobsen, E. N., Pfaltz, A., Yamamoto, H., Eds.; Springer-Verlag: Berlin, 1999; Vol. I, pp 121−182. (d) *Asymmetric Catalysis in Organic Synthesis*; Noyori, R., Ed.; Wiley: New York, 1994. (e) *Applied Homogeneous Catalysis with Organometallic Compounds*, 2nd ed.; Cornils, B., Herrmann, W. A., Eds.; Wiley-VCH: Weinheim, 2002.

(2) For recent reviews, see: (a) Källström, K.; Munslow, I.; Andersson, P. G. *Chem.-Eur. J.* **2006**, *12*, 3194. (b) Roseblade, S. J.; Pfaltz, A. *Acc. Chem. Res.* **2007**, *40*, 1402. (c) Church, T. L.; Andersson, P. G. *Coord. Chem. Rev.* **2008**, *252*, 513. (d) Cui, X.; Burgess, K. *Chem. Rev.* **2005**, *105*, 3272. (e) Pàmies, O.; Andersson, P. G.; Diéguez, M. *Chem.-Eur. J.* **2010**, *16*, 14232.

(3) Chelating oxazoline−carbene ligands, mainly developed by Burgess and co-workers, have also been successfully used and also to a less extent chiral diphosphines. See, for instance: (a) Perry, M. C.; Cui, X.; Powell, M. T.; Hou, D. R.; Reibenspies, J. H.; Burgess, K. *J. Am. Chem. Soc.* **2003**, *125*, 113. (b) Cui, X.; Burgess, K. *J. Am. Chem. Soc.* **2003**, *125*, 14212. (c) Cui, X.; Ogle, J. W.; Burgess, K. *Chem. Commun.* **2005**, 672. (d) Zhao, J.; Burgess, K. *J. Am. Chem. Soc.* **2009**, *131*, 13236. (e) Co, T. T.; Kim, T. J. *Chem. Commun.* **2006**, 3537. (f) Forman, G. S.; Ohkuma, T.; Hems, W. P.; Noyori, R. *Tetrahedron Lett.* **2000**, *41*, 9471.

(4) See, for instance: (a) Perry, M. C.; Cui, X.; Powell, M. T.; Hou, D.-R.; Reibenspies, J. H.; Burgess, K. *J. Am. Chem. Soc.* **2003**, *125*, 5391. (b) Blankestein, J.; Pfaltz, A. *Angew. Chem., Int. Ed.* **2001**, *40*, 4445. (c) Kaiser, S.; Smidt, S. P.; Pfaltz, A. *Angew. Chem., Int. Ed.* **2006**, *45*, 5194. (d) Källström, K.; Hedberg, C.; Brandt, P.; Bayer, P.; Andersson, P. G. *J. Am. Chem. Soc.* **2004**, *126*, 14308. (e) Engman, M.; Diesen, J. S.; Paptchikhine, A.; Andersson, P. G. *J. Am. Chem. Soc.* **2007**, *129*, 4536. (f) Trifonova, A.; Diesen, J. S.; Andersson, P. G. *Chem.-Eur. J.* **2006**, *12*, 2318. (g) Menges, G.; Pfaltz, A. *Adv. Synth. Catal.* **2002**, *334*, 4044. (h) Drury, W. J., III; Zimmermann, N.; Keenan, M.; Hayashi, M.; Kaiser, S.; Goddard, R.; Pfaltz, A. *Angew. Chem., Int. Ed.* **2004**, *43*, 70. (i) Hedberg, C.; Källström, K.; Brandt, P.; Hansen, L. K.; Andersson, P. G. *J. Am. Chem. Soc.* **2006**, *128*, 2995. (j) Franzke, A.; Pfaltz, A. *Chem.-Eur. J.***2011**, *17*, 4131. (k) Tang, W.; Wang, W.; Zhang, X. *Angew. Chem., Int. Ed.* **2003**, *42*, 943. (l) Hou, D.-R.; Reibenspies, J.; Colacot, T. J.; Burgess, K. *Chem.-Eur. J.* **2001**, *7*, 5391. (m) Cozzi, P. G.; Menges, F.; Kaiser, S. *Synlett* **2003**, 833. (n) Lightfoot, A.; Schnider, P.; Pfaltz, A. *Angew. Chem., Int. Ed.* **1998**, *37*, 2897. (o) Menges, F.; Neuburger, M.; Pfaltz, A. *Org. Lett.* **2002**, *4*, 4713. (p) Liu, D.; Tang, W.; Zhang, X. *Org. Lett.* **2004**, *6*, 513. (q) Lu, S.-M.; Bolm, C. *Angew. Chem., Int. Ed.* **2008**, *47*, 8920. (r) Lu, W.-J.; Chen, Y.-W.; Hou, X.-L. *Adv. Synth. Catal.* **2010**, *352*, 103. (s) Paptchikhine, A.; Cheruku, P.; Engman, M.; Andersson, P. G. *Chem. Commun.* **2009**, 5996.

(5) (a) Diéguez, M.; Mazuela, J.; Pàmies, O.; Verendel, J. J.; Andersson, P. G. *J. Am. Chem. Soc.* **2008**, *130*, 7208. (b) Diéguez, M.; Mazuela, J.; Pàmies, O.; Verendel, J. J.; Andersson, P. G. *Chem. Commun.* **2008**, 3888. (c) Mazuela, J.; Verendel, J. J.; Coll, M.; Schäffner, B.; Börner, A.; Andersson, P. G.; Pàmies, O.; Diéguez, M. M. *J. Am. Chem. Soc.* **2009**, *131*, 12344. (d) Mazuela, J.; Paptchikhine, A.; Pàmies, O.; Andersson, P. G.; Diéguez, M. *Chem.-Eur. J.* **2010**, *16*, 4567.

(6) One of the limitations of using sugars as precursors for ligands is that often only one of the enantiomers is readily available. However, this limitation can be overcome by the rational design of *pseudo*-enantiomeric ligands. See, for example: (a) RajanBabu, T. V.; Ayers, T. A.; Casalnuovo, A. L. *J. Am. Chem. Soc.* **1994**, *116*, 4101. (b) RajanBabu, T. V.; Ayers, T. A.; Halliday, G. A.; You, K. K.; Calabrese, J. C. *J. Org. Chem.* **1997**, *62*, 6012. (c) Khiar, N.; Navas, R.; Suárez, B.; Álvarez, E.; Fernández, I. *Org. Lett.* **2008**, *10*, 3697. (d) Nakano, H.; Yokohama, J.; Okuyama, Y.; Fujita, R.; Hongo, H. *Tetrahedron: Asymmetry* **2003**, *14*, 2361. (e) Ruffo, F.; Del Lito, R.; De Roma, A.; D'Errico, A.; Magnolia, S. *Tetrahedron: Asymmetry* **2006**, *17*, 2265.

(7) (a) Mata, Y.; Pàmies, O.; Diéguez, M.; Claver, C. *Adv. Synth. Catal.* **2005**, *347*, 1943. (b) Mata, Y.; Pàmies, O.; Diéguez, M. *Chem.-Eur. J.* **2007**, *13*, 3296. (c) Mata, Y.; Pàmies, O.; Diéguez, M. *Adv. Synth. Catal.* **2009**, *351*, 3217.

(8) Yonehara, K.; Jashizume, T.; Mori, K.; Ohe, K.; Uemura, S. *J. Org. Chem.* **1999**, *64*, 9374.

(9) For the preparation of [Ir(cod)(**L5j**)]BAr_F, the anion exchange has been performed at low temperature (0 °C) without the presence of water.

(10) The rapid ring inversions (tropoisomerization) in the biaryl phosphite moiety are usually stopped upon coordination to the metal center. See, for example: (a) Buisman, G. J. H.; van der Veen, L. A.; Klootwijk, A.; de Lange, W. G. J.; Kamer, P. C. J.; van Leeuwen, P. W. N. M.; Vogt, D. *Organometallics* **1997**, *16*, 2929. (b) Diéguez, M.; Pàmies, O.; Ruiz, A.; Claver, C.; Castillón, S. *Chem.-Eur. J.* **2001**, *7*, 3086. (c) Pàmies, O.; Diéguez, M.; Net, G.; Ruiz, A.; Claver, C. *Organometallics* **2000**, *19*, 1488. (d) Pàmies, O.; Diéguez, M.; Net, G.; Ruiz, A.; Claver, C. *J. Org. Chem.* **2001**, *66*, 8364. (e) Pàmies, O.; Diéguez, M. *Chem.-Eur. J.* **2008**, *14*, 944.

(11) (a) Rovner, E. S.; Wein, A. *J. Eur. Urol.* **2002**, *41*, 6. (b) Wefer, J.; Truss, M. C.; Jonas, U. *World J. Urol.* **2001**, *19*, 312. (c) Hills, C. J.; Winter, S. A.; Balfour, J. A. *Drugs* **1998**, *55*, 813. (d) McRae, A. L.; Brady, K. T. *Expert Opin. Pharmacother.* **2001**, *2*, 883. (e) Gordaliza, M.; García, P. A.; Miguel del Corral, J. M.; Castro, M. A.; Gómez-Zurita, M. A. *Toxicon* **2004**, *44*, 441.

(12) Tolstoy, P.; Engman, M.; Paptchikhine, A.; Bergquist, J.; Church, T. L.; Leung, A. W.-M.; Andersson, P. G. *J. Am. Chem. Soc.* **2009**, *131*, 8855.

(13) For successful application of Ir-catalysts, see: (a) McIntyre, S.; Hörmann, E.; Menges, F.; Smidt, S. P.; Pfaltz, A. *Adv. Synth. Catal.* **2005**, *347*, 282.(b) Reference 4b.

(14) For successful applications of Sm-, Ru-, and Rh-complexes, see: (a) Conticello, V. P.; Brard, L.; Giardello, M. A.; Tsuji, Y.; Sabat, M.; Stern, C. L.; Marks, T. J. *J. Am. Chem. Soc.* **1992**, *114*, 2761. (b) Giardello, M. A.; Conticello, V. P.; Brard, L.; Gagné, M. R.; Marks, T. J. *J. Am. Chem. Soc.* **1994**, *116*, 10241.(c) Reference 3e. (d) Reference 3f.

(15) (a) Fessard, T. C.; Andrews, S. P.; Motoyohsi, H.; Carreira, E. *Angew. Chem., Int. Ed.* **2007**, *46*, 9331. (b) Prat, L.; Dupas, G.; Duflos, J.; Quéguiner, G.; Bourguignon, J.; Levacher, V. *Tetrahedron Lett.* **2001**, *42*, 4515. (c) Wilkinson, J. A.; Rossington, S. B.; Ducki, S.; Leonard, J.; Hussain, N. *Tetrahedron* **2006**, *62*, 1833.

(16) (a) Okamoto, K.; Nishibayashi, Y.; Uemura, S.; Toshimitsu, A. *Angew. Chem., Int. Ed.* **2005**, *44*, 3588. (b) Hatanaka, Y.; Hiyama, T. *J. Am. Chem. Soc.* **1990**, *112*, 7793.

(17) See, for instance: (a) Abate, A.; Brenna, E.; Fuganti, C.; Gatti, G. G.; Givenzana, T.; Malpezzi, L.; Serra, S. *J. Org. Chem.* **2005**, *70*, 1281. (b) Drescher, K.; Haupt, A.; Unger, L.; Rutner, S. C.; Braje, W.; Grandel, R.; Henry, C.; Backfisch, G.; Beyerbach, A.; Bisch, W. WO Patent 2006/040182 A1, 2006.

(18) See, for instance: (a) Schlosser, M. *Angew. Chem., Int. Ed.* **1998**, *37*, 1496. (b) Smart, B. E. *J. Fluorine Chem.* **2001**, *109*, 3.(c) *Asymmetric Fluoroorganic Chemistry: Synthesis, Application and Future Directions*; Ramachandran, P. V., Ed.; American Chemical Society: Washington, DC, 2000. (d) A special issue has been devoted to "Fluorine in the Life Sciences". *ChemBioChem* **2004**, *5*, 559.

(19) See, for instance: (a) Fleming, I.; Barbero, A.; Walter, D. *Chem. Rev.* **1997**, *97*, 2063. (b) Jones, G. R.; Landais, Y. *Tetrahedron* **1996**, *52*, 7599. (c) Bains, W.; Tacke, R. *Curr. Opin. Drug Discovery Dev.* **2003**, *6*, 526.

(20) (a) Feldgus, S.; Landis, C. R. *J. Am. Chem. Soc.* **2000**, *122*, 12714. (b) Donoghue, P. J.; Helquist, P.; Norrby, P.-O.; Wiest, O. *J. Am. Chem. Soc.* **2009**, *131*, 410.

(21) (a) Roseblade, S. J.; Pfaltz, A. *C. R. Chim.* **2007**, *10*, 178. (b) Vazquez-Serrano, L. D.; Owens, B. T.; Buriak, J. M. *Chem. Commun.* **2002**, 2518.

(22) (a) Cui, X.; Fan, Y.; Hall, M. B.; Burgess, K. *Chem.-Eur. J.* **2005**, *11*, 6859. (b) Fan, Y.; Cui, X.; Burgess, K.; Hall, M. B. *J. Am. Chem. Soc.* **2004**, *126*, 16688. (c) Brandt, P.; Hedberg, C.; Andersson, P. G. *Chem.-Eur. J.* **2003**, *9*, 339.

(23) Church, T. L.; Rasmussen, T.; Andersson, P. G. *Organometallics* **2010**, *29*, 6769.

(24) Recently, the group of Hopmann et al. has performed a computationally study using a phosphine−oxazoline (PHOX)-based iridium catalyst, which indicates that the hydrogenation of **S1** follows the 3/5-Meta pathway. See: Hopmann, K. H.; Bayer, A. *Organometallics* **2011**, *30*, 2483.

(25) *Jaguar*, version 7.0; Schrödinger, LLC: New York, 2010; http://www.schrodinger.com/.

(26) (a) Becke, A. D. *J. Chem. Phys.* **1993**, *98*, 5648. (b) Lee, C.; Yang, W.; Parr, R. G. *Phys. Rev. B* **1988**, *37*, 785.

(27) Grimme, S.; Antony, J.; Ehrlich, S.; Krieg, H. *J. Chem. Phys.* **2010**, *132*, 154104.

(28) The rest of the possible isomers generated from considering the hydride attack to the less substituted carbon of the olefin have not been considered, because it has been previously demonstrated that they proceed with higher energies. See ref 4i.

(29) Buisman, G. J. H.; Kamer, P. C. J.; van Leeuwen, P. W. N. M. *Tetrahedron: Asymmetry* **1993**, *4*, 1625.

(30) Hay, P. J.; Wadt, W. R. *J. Chem. Phys.* **1985**, *82*, 299.

(31) (a) Tannor, D. J.; Marten, B.; Murphy, R.; Friesner, R. A.; Sitkoff, D.; Nicholls, A.; Honig, B.; Ringnalda, M.; Goddard, W. A. *J. Am. Chem. Soc.* **1994**, *116*, 11875. (b) Marten, B.; Kim, K.; Cortis, C.; Friesner, R. A.; Murphy, R. B.; Ringnalda, M. N.; Sitkoff, D.; Honig, B. *J. Phys. Chem.* **1996**, *100*, 11775.